Appendix A: Counterexample

Straightforwardly adopting the labeling algorithms proposed in Baum et al. (2019) and Froger et al. (2019) to our problem setting yields an algorithm with a slightly modified label representation. Specifically, cost profiles track only the *last* visited station in these works. Accordingly, intermediate charging is not possible such that realizing a charging opportunity at i when propagating ℓ along (i,j) creates new labels according to the station replacement operation (Section 3.5) only. Specifically, the algorithm creates a set of new labels $\{\ell \underset{(i,j)}{\overset{f(i)}{\leftarrow}} c \mid \forall c \in \mathcal{B}(\psi_\ell)\} \cup \{\ell \underset{(i,j)}{\leftarrow} /\}$ based on the breakpoints of cost profile ψ_ℓ at target vertex j.

The following example illustrates a case where this approach does not yield an optimal solution: consider a planning horizon of two periods $\mathcal{P}_1, \mathcal{P}_2$ of duration $\xi = 5$ with energy prices $e_{\mathcal{P}_1} = 10c$ and $e_{\mathcal{P}_2} = c$, a single service operation with consumption q, and a single charger f with constant charging rate $\frac{q}{8}$. For the sake of simplicity, we ignore battery degradation in this example and assume zero fixed costs for each arc in the time-expanded network. The optimal path through this network spends $3 \cdot 10c$ on charging at vertex $(\mathcal{P}_1, f)$ and $5 \cdot c$ at $(\mathcal{P}_2, f)$, such that the minimal cost is $3 \cdot 10c + 5 \cdot c$. According to (Baum et al. 2019, Froger et al. 2019), a visit to vertex $(\mathcal{P}_1, f)$ generates a single label with cost profile $\psi_{\ell_1}(c) = \frac{c}{10} \forall c \in [0,5]$. Realizing the second charging opportunity at vertex $(\mathcal{P}_2, f)$ then creates two labels, one for each breakpoint of ψ_{ℓ_1}, i.e., $\ell_2 \coloneqq \ell_1 \underset{(i,j)}{\overset{f(i)}{\leftarrow}} 0$ and $\ell_3 \coloneqq \ell_1 \underset{(i,j)}{\overset{f(i)}{\leftarrow}} 5 \cdot 10c$. Here, ℓ_2 is infeasible as $q_{\max}(\psi_{\ell_2}) = \frac{5}{8} q < q$ and ℓ_3 is not optimal: $\psi_{\ell_3}^{-1}(q) = 5 \cdot 10c + 3c > 3 \cdot 10c + 5c$.

Appendix B: Proofs

PROPOSITION 1. *The slope of a cost profile $\psi_{\ell'}$ obtained from $\ell' \coloneqq \ell \underset{(i,j)}{\leftarrow} \tau$ can only be negative at $c \in [c_{\min}(\psi_{\ell'}), c_{\max}(\psi_{\ell'})]$ if for $q' \coloneqq \Phi_{f(i)}(\Phi_{f(i)}^{-1}(\psi_{\ell'}^{-1}(c)) - \tau)$, $\angle_{\psi_\ell^{-1}}(q') < \angle_{\psi_{i,j}^{-1}}(q')$ holds.*

Proof: we first observe that Term 12.1 is never negative as $\Phi_{f(i)}$ is piecewise linear and concave, which, together with $\Phi_{f(i)}^{-1}(q) - \tau \leq \Phi_{f(i)}^{-1}(q)$, implies $\angle_{\Phi_{f(i)}}(\Phi_{f(i)}^{-1}(q) - \tau) \geq \angle_{\Phi_{f(i)}}(\Phi_{f(i)}^{-1}(q))$:

$$\angle_{\Phi_{f(i)}}(\Phi_{f(i)}^{-1}(q) - \tau) \cdot \angle_{\Phi_{f(i)}^{-1}}(q) = \frac{\angle_{\Phi_{f(i)}}(\Phi_{f(i)}^{-1}(q) - \tau)}{\angle_{\Phi_{f(i)}}(\Phi_{f(i)}^{-1}(q))} \geq 1.$$

As $\angle_{\psi_{i,j}^{-1}}$ is non-negative, we have $\angle_{\psi_{\ell'}^{-1}}(q') < 0$, which implies $\angle_{\psi_\ell^{-1}}(q') < \angle_{\psi_{i,j}^{-1}}(q')$. □

PROPOSITION 2. *For any c on a decreasing segment $[c', c' + \epsilon]$ with $\epsilon > 0$ of some cost profile $\psi_{\ell'}$ obtained from $\ell' \coloneqq \ell \underset{(i,j)}{\leftarrow} \tau$, there exists some $\ell'' \in \mathcal{L}_j \setminus \{\ell'\}$ such that $\psi_{\ell''}(c) \geq \psi_{\ell'}(c)$.*

Proof: let there be some c where $\psi_{\ell'}$ is decreasing. Further let $q \coloneqq \psi_{\ell'}^{-1}(c)$. Since $\psi_{\ell'}$ is decreasing on $[c', c' + \epsilon]$, we have $c_{\min}(\psi_{\ell'}) < c < c_{\max}(\psi_{\ell'})$ such that there exists some $\ell'' \coloneqq \ell \underset{(i,j)}{\overset{f(i)}{\leftarrow}} c''$ with $q_{\max}(\psi_{\ell''}) = q$. As we have $\angle_{\psi_\ell^{-1}}(q') < \angle_{\psi_{i,j}^{-1}}(q')$ for $q' \coloneqq \psi_{\ell''}^{-1}(c'')$ (Proposition 1), we can apply the same reasoning as in the proof of Theorem 1 (Case 2.2) and argue that there exists some set of labels $\mathcal{L}' \subseteq \mathcal{L}_j \setminus \{\ell'\}$ such that $\mathcal{L}' \geq \psi_{\ell'}(c)$.

□

THEOREM 1. *For any charging arc (i,j) and label $\ell_i \in \mathcal{L}_i$, the set of labels*

$$\mathcal{L}' \coloneqq \{\ell_j, \ell_i \underset{(i,j)}{\leftarrow} \xi\} \cup \{\ell_i \overset{f(i)}{\underset{(i,j)}{\leftarrow}} c \mid \forall c \in \mathcal{B}(\psi_{\ell_i})\},$$

with $\ell_j \coloneqq \ell_i \underset{(i,j)}{\leftarrow}$ / dominates any label

$$\ell' \in \{\ell_i \overset{f(i)}{\underset{(i,j)}{\leftarrow}} c \mid c \in [c_{\min}(\psi_{\ell_i}), c_{\max}(\psi_{\ell_i})]\} \cup \{\ell_i \underset{(i,j)}{\leftarrow} \tau \mid 0 \le \tau \le \xi\} \setminus \mathcal{L}'.$$

Proof: assume the contrary, i.e., that there exists some ℓ' not dominated by $\mathcal{L}'$. Then there exists some $c \in \mathbb{R}$ such that $\psi_{\ell'}(c) > \max_{\ell'' \in \mathcal{L}'}\{\psi_{\ell''}(c)\}$.

Case 1: $c < c_{\min}(\psi_{\ell'})$.

Then $\psi_{\ell'}(c) = -\infty \le \max_{\psi_{\ell''} \in \mathcal{L}'}\{\ell''(c)\}$ holds by definition.

Case 2: $c_{\min}(\psi_{\ell'}) \le c \le c_{\max}(\psi_{\ell'})$.

W.l.o.g., we assume $\ell' = \ell_i \overset{f(i)}{\underset{(i,j)}{\leftarrow}} c'$ for some c' and let $c'_j \coloneqq c' + c_{i,j}$ and $q' \coloneqq \psi_{\ell_i}(c') = \psi_{\ell_j}(c'_j)$. Recall from Section 3.5 that

$$\begin{aligned}\psi_{\ell'}(c) &= \psi_{\ell_i}(c') + c_{i,j} + \Delta c^{-1}_{p(i),f(i)}\langle q'\rangle(c - c_{i,j} - c')\\ &= \psi_{\ell_j}(c'_j) + \Delta c^{-1}_{p(i),f(i)}\langle q'\rangle(c - c_{i,j} - c')\\ &= \psi_{\ell_j}(c'_j) + \Delta c^{-1}_{p(i),f(i)}\langle q'\rangle(c - c'_j).\end{aligned}$$

Case 2.1: $\angle_{\psi_{\ell_j}}(c'_j) \ge \angle_{\psi^{\rightarrow}_{i,j}}(c'_j)$.

Let $\ell'' \coloneqq \ell_i \overset{f(i)}{\underset{(i,j)}{\leftarrow}} c''$, with $c'' = \min\{c \mid c \in \mathcal{B}(\psi_{\ell_i}) \wedge c \ge c'\}$, and let $c''_j \coloneqq c'' + c_{i,j}$ such that

$$\begin{aligned}\psi_{\ell''}(c) &= \psi_{\ell_i}(c') + c_{i,j} + \Delta c^{-1}_{p(i),f(i)}\langle q''\rangle(c - c_{i,j} - c'')\\ &= \psi_{\ell_j}(c''_j) + \Delta c^{-1}_{p(i),f(i)}\langle q''\rangle(c - c_{i,j} - c'')\\ &= \psi_{\ell_j}(c''_j) + \Delta c^{-1}_{p(i),f(i)}\langle q''\rangle(c - c''_j).\end{aligned}$$

We argue that ℓ'' exists and $\ell'' \in \mathcal{L}'$ holds since $c' \in [c_{\min}(\psi_{\ell_i}), c_{\max}(\psi_{\ell_i})]$.

Case 2.1.1: $c_{\min}(\psi_{\ell'}) \le c \le c_{\min}(\psi_{\ell''})$.

Then we have $c_{\min}(\psi_{\ell_j}) \le c < c_{\min}(\psi_{\ell''}) \le c_{\max}(\psi_{\ell_j})$. From the definition of ℓ'', it further follows that $\angle_{\psi_{\ell_j}}$ is constant on $[c'_j, c]$. Hence, we get

$$\begin{aligned}\psi_{\ell_j}(c) &= \psi_{\ell_j}(c'_j) + \psi_{\ell_j}(c) - \psi_{\ell_j}(c'_j)\\ &= \psi_{\ell_j}(c'_j) + \angle_{\psi_{\ell_j}}(c'_j)\cdot(c - c'_j)\\ &\overset{(\star)}{\ge} \psi_{\ell_j}(c'_j) + \angle_{\psi_{i,j}}(c'_j)\cdot(c - c'_j)\\ &= \psi_{\ell'}(c),\end{aligned}$$

which contradicts our assumption. Here, $(\star)$ holds as $\angle_{\psi_{\ell_j}}(c'_j) \ge \angle_{\psi^{\rightarrow}_{i,j}}(c'_j)$.

Case 2.1.2 : $c_{\min}(\psi_{\ell''}) < c \leq c_{\max}(\psi_{\ell'})$.

We note that $\Delta q \coloneqq \psi_{\ell''}(c''_j) - \psi_{\ell'}(c''_j) \geq 0$ holds by Case 2.1.1, such that it holds that $\Delta c \coloneqq \psi_{\ell'}^{-1}(q'') - c''_j \geq 0$. Hence, for $c < c''_j + \Delta c$, we have $\psi_{\ell''}(c) \geq \psi_{\ell'}(c)$ since $\Delta c^{-1}_{p(i),f(i)}\langle q\rangle(\cdot)$ are concave for $q \in [\mathtt{SoC}_{\min}, \mathtt{SoC}_{\max}]$ (cf. Section 3.5). Using the same argument for inequality $(\star)$, we get the following for $c \geq c''_j + \Delta c$:

$$\begin{aligned}\psi_{\ell'}(c) &= q' + \Delta c^{-1}_{p(i),f(i)}\langle q'\rangle(c - c'_j)\\ &= q'' + \Delta c^{-1}_{p(i),f(i)}\langle q''\rangle(c - (c''_j + \Delta c))\\ &\overset{(\star)}{\leq} q'' + \Delta c^{-1}_{p(i),f(i)}\langle q''\rangle(c - c''_j)\\ &= \psi_{\ell''}(c),\end{aligned}$$

which contradicts the assumption. See Figure 1a for an illustration.

Case 2.2: $\angle_{\psi_{\ell_j}}(c'_j) < \angle_{\psi^{\rightarrow}_{i,j}}(c'_j)$.

Let $\ell'' \coloneqq \ell_i \overset{f(i)}{\underset{(i,j)}{\leftarrow}} c''$, with $c'' = \max\{c \mid c \in \mathcal{B}(\psi_{\ell_i}) \wedge c \leq c'\}$, and let $c''_j \coloneqq c'' + c_{i,j}$ such that $\psi_{\ell''}(c) = \psi_{\ell_j}(c''_j) + \Delta c^{-1}_{p(i),f(i)}\langle q''\rangle(c - c''_j)$.

Case 2.2.1: $\psi_{\ell'}(c) \leq q_{\max}(\psi_{\ell''})$.

It follows from the definition of ℓ'' that $\angle_{\psi_{\ell_j}}$ is constant on $[c'_j, c''_j]$. Then, analogous to Case 2.1.1, we have

$$\begin{aligned}\psi_{\ell''}(c'_j) &= \psi_{\ell''}(c''_j) + \psi_{\ell''}(c'_j) - \psi_{\ell''}(c''_j)\\ &\overset{(\star)}{\geq} \psi_{\ell''}(c''_j) + \angle_{\psi^{\rightarrow}_{i,j}}(c'_j)\cdot(c'_j - c''_j)\\ &\overset{(\star\star)}{\geq} \psi_{\ell''}(c''_j) + \angle_{\psi_{\ell_j}}(c'_j)\cdot(c'_j - c''_j)\\ &\overset{(\star\star\star)}{=} \psi_{\ell'}(c''_j) + \angle_{\psi_{\ell_j}}(c'_j)\cdot(c'_j - c''_j)\\ &= \psi_{\ell'}(c'_j).\end{aligned}$$

Here, $(\star)$ follows from the concavity of $\psi^{\rightarrow}_{i,j}$, i.e., $\angle_{\psi^{\rightarrow}_{i,j}}(c''_j) \geq \angle_{\psi^{\rightarrow}_{i,j}}(c'_j)$, $(\star\star)$ follows from $\angle_{\psi_{\ell_j}}(c'_j) < \angle_{\psi_{i,j}}(c'_j)$, and $(\star\star\star)$ holds since $\angle_{\psi_{\ell_j}}$ is constant on $[c''_j, c'_j]$ by the definition of c'_j and c''_j.

Concluding, $\Delta q \coloneqq \psi_{\ell''}(c'_j) - q' \geq 0$ holds, which implies $\Delta c \coloneqq \psi_{\ell'}^{-1}(\psi_{\ell''}(c'_j)) - \psi_{\ell'}^{-1}(q') \geq 0$, such that, analogous to Case 2.1.2, we get $\psi_{\ell''}(c) \geq \psi_{\ell'}(c)$ for $c + \Delta c < c'_j$ due to the concavity of $\Delta c^{-1}_{p(i),f(i)}\langle q\rangle(\cdot)$ (cf. Section 3.5). Furthermore, for $c + \Delta c \geq c'_j$, it holds that

$$\begin{aligned}\psi_{\ell''}(c) &= q'' + \Delta c^{-1}_{p(i),f(i)}\langle q''\rangle(c - c'_j)\\ &= q' + \Delta c^{-1}_{p(i),f(i)}\langle q'\rangle(c - c'_j + \Delta c)\\ &\geq q' + \Delta c^{-1}_{p(i),f(i)}\langle q'\rangle(c - c'_j)\\ &= \psi_{\ell'}(c),\end{aligned}$$

which contradicts the assumption. See Figure 1b for an illustration.

Case 2.2.2: $\psi_{\ell'}(c) > q_{\max}(\psi_{\ell''})$.

Let $\ell_\xi \coloneqq \ell_i \underset{(i,j)}{\leftarrow} \xi$ and $q \coloneqq \psi_{\ell'}(c)$. Further let $\ell''' \coloneqq \ell_i \overset{f(i)}{\underset{(i,j)}{\leftarrow}} c'''$ such that $q_{\max}(\psi_{\ell'''}) = q$. The existence of ℓ''' follows straightforwardly from $c \leq c_{\max}(\psi_{\ell'})$ and the existence of ℓ'. Let $c'''_j \coloneqq c''' + c_{i,j}$ and $q''' \coloneqq \psi_{\ell'''}(c'''_j)$. Note that $c'' \leq c''' \leq c'$, and thus $c''_j \leq c'''_j \leq c'_j$, since the definition of c'' implies that $\angle_{\psi_{\ell_i}}$ is constant on $[c'', c']$. Hence, analogous to Case 2.2.1, we get $\psi_{\ell'''}(c) \geq \psi_{\ell'}(c)$. With this in mind, we recall from Equation 8 that

$$\begin{aligned}
\psi^{-1}_{\ell'''}(q) &= \psi^{-1}_{\ell'''}(q_{\max}(\psi_{\ell'''})) = c'''_j + \Delta c_{p(i),f(i)}\langle q'''\rangle(\Phi_{f(i)}(q''', \xi) - q''') \\
&= \psi^{-1}_{\ell_j}(q''') + \Delta c_{p(i),f(i)}\langle q'''\rangle(\Phi_{f(i)}(q''', \xi) - q''') \\
&= \psi^{-1}_{\ell_i}(q''') + c_{i,j} + \Delta c_{p(i),f(i)}\langle q'''\rangle(\Phi_{f(i)}(q''', \xi) - q''').
\end{aligned}$$

Recall that $q \coloneqq \psi_{\ell'}(c) = \Phi_{f(i)}(q''', \xi)$, such that substituting q yields

$$\begin{aligned}
&\psi^{-1}_{\ell_i}(q''') + c_{i,j} + \Delta c_{p(i),f(i)}\langle q'''\rangle(\Phi_{f(i)}(q''', \xi) - q''') \\
&= \psi^{-1}_{\ell_i}(q''') + c_{i,j} + \Delta c_{p(i),f(i)}\langle q'''\rangle(q - q''') \\
&\overset{(\star)}{=} \psi^{-1}_{\ell_i}(q''') + c_{i,j} + (\Delta c_{p(i),f(i)}\langle 0\rangle(q) - \Delta c_{p(i),f(i)}\langle 0\rangle(q''')) \\
&= \psi^{-1}_{\ell_i}(q''') + c_{i,j} + (\psi^{-1}_{i,j}(q) - \psi^{-1}_{i,j}(q''')) \\
&= \psi^{-1}_{\ell_\xi}(q).
\end{aligned}$$

Here, $(\star)$ holds since

$$\begin{aligned}
\Delta c_{p(i),f(i)}\langle q'''\rangle(q - q''') &= e_p \cdot (q - q''') + \Upsilon(q''', q''' + q - q''') \\
&= e_p \cdot (q - q''') + \Upsilon(q''' + q - q''') - \Upsilon(q''') \\
&= e_p \cdot (q - q''') + \Upsilon(q) - \Upsilon(q''') \\
&= (e_p \cdot q + \Upsilon(q) - \Upsilon(0)) - (e_p \cdot q''' + \Upsilon(q''') - \Upsilon(0)) \\
&= (e_p \cdot q + \Upsilon(0, q)) - (e_p \cdot q''' + \Upsilon(0, q''')) \\
&= \Delta c_{p(i),f(i)}\langle 0\rangle(q) - \Delta c_{p(i),f(i)}\langle 0\rangle(q''').
\end{aligned}$$

Concluding, we have $\psi^{-1}_{\ell_\xi}(q) = \psi^{-1}_{\ell'''}(q)$ and $\psi_{\ell'''}(c) \geq \psi_{\ell'}(c)$ such that $\psi^{-1}_{\ell_\xi}(q) = \psi^{-1}_{\ell'''}(q) \leq \psi^{-1}_{\ell'}(q)$, which contradicts the assumption. See Figure 1c for an illustration.

Case 3: $c \geq c_{\max}(\psi_{\ell'})$.

Case 2 implies that $\exists \ell'' \in \mathcal{L}' : \psi_{\ell''}(c_{\max}(\psi_{\ell'})) \geq q_{\max}(\psi_{\ell'})$. Hence, as $\psi_{\ell'}(c) = q_{\max}(\psi_{\ell'})$ by definition, we get $\psi_{\ell''}(c_{\max}(\psi_{\ell'})) \geq q_{\max}(\psi_{\ell'})$, which contradicts the assumption.

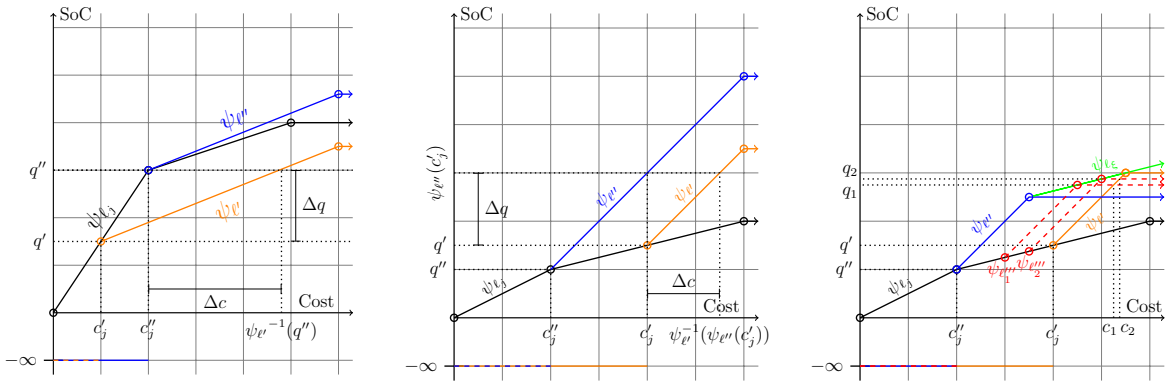

(a) $\angle_{\psi_{\ell_j}}(c'_j) \geq \angle_{\psi_{i,j}}(c'_j)$ (Case 2.1).

Note. Δc corresponds to the additional cost incurred by using vertex i to recharge up to the state of charge (SoC) at which ℓ'' stops charging using the charging opportunity captured by the previous label. As the previous charging opportunity provides a lower price, Δc is positive.

(b) $\angle_{\psi_{\ell_j}}(c'_j) < \angle_{\psi_{i,j}}(c'_j)$, $\psi_{\ell'}(c) \leq q_{\max}(\psi_{\ell''})$ (Case 2.2.1).

Note. Here, Δc corresponds to the cost saved by using i to charge up to the arrival SoC of ℓ' at j. Δc is positive as station i provides a lower charging price in this case.

(c) $\angle_{\psi_{\ell_j}}(c'_j) < \angle_{\psi_{i,j}}(c'_j)$, $\psi_{\ell'}(c) > q_{\max}(\psi_{\ell''})$ (Case 2.2.2).

Note. c_1 and c_2 provide example values for c. The red dashed lines illustrate the corresponding cost profiles $\psi_{\ell'''_1}$ and $\psi_{\ell'''_2}$, respectively. The green profile illustrates charging intermediately. Note that, for the sake of simplicity, we show only the segment of ψ_{ℓ_ξ} relevant to this proof.

Figure 1: Illustration of cases 2.1 and 2.2 in the proof of Theorem 1.

Concluding, for any $c \in \mathbb{R}$, there exists a $\ell'' \in \mathcal{L}'$, such that $\psi_{\ell''}(c) \geq \psi_{\ell'}(c)$. Hence, $\max_{\ell'' \in \mathcal{L}'}\{\ell''(c)\} \geq \psi_{\ell'}(c)$, and Theorem 1 holds. □

PROPOSITION 3. *Let σ be a fractional basic feasible solution to the restricted master problem (RMP). Then it holds that $\exists (p,f) \in \mathcal{P} \times \mathcal{F}$ such that $\sum_{x^k_\omega \in \sigma} x^k_\omega \boldsymbol{A}^\omega_{p,f} = C_f$, and there exist at least two $x^k_\omega \in \sigma$ with $0 < x^k_\omega < 1$.*

Proof: Assume the contrary, i.e., that there exists schedules $\omega_1, \ldots, \omega_n$ in basic feasible $\sigma = (x^{k_1}_{\omega_1}, \ldots, x^{k_n}_{\omega_n})$ with $0 < x^k_\omega < 1$, and $\sum_{x^k_\omega \in \sigma} x^k_\omega \boldsymbol{A}^\omega_{p,f} < C_f$. Let $k' \in \mathcal{K}$ such that $\exists \omega_i, \omega_j \in \mathcal{A}_{k'}$ with $i \neq j$ and $0 < x^{k'}_{\omega_i} \leq x^{k'}_{\omega_j} < 1$ in σ. Here, convexity Constraints (2c) ensure the existence of such ω_i and ω_j. As charger capacity Constraints (2b) are non-binding, there exists $\epsilon > 0$ such that $\sigma' = (x^{k_1}_{\omega_1}, \ldots, x^{k'}_{\omega_i} + \epsilon, \ldots, x^{k'}_{\omega_j} - \epsilon, \ldots, x^{k_n}_{\omega_n})$ is feasible. This implies that σ is not basic and thus contradicts the assumption. □

Appendix C: Fundamentals

The following sections detail the methodology behind and the derivation of charging functions Φ_f and (cumulative) wear density function (WDF) $\widetilde{\Upsilon}$: we first provide an overview of the electro-chemical fundamentals of the charging process and discuss a charging scheme that prevents overcharging and

thus critically damaging the battery's internals in Section C.1. Afterwards, we show how to model this charging scheme in functions Φ_f (Section C.2). Finally, Section C.3 details how we capture battery health considerations in our optimization problem. For an in-depth review of battery modeling for electric commercial vehicles (ECVs) in particular and electro-chemical cells in general, we refer to Pelletier et al. (2017) and Franco (2015).

C.1. The Constant Current-Constant Voltage charging scheme

A battery's capacity can be measured in several units: Ampere-hours, Coulombs, and kWh, each proper in different application cases. To avoid confusion arising from handling these technicalities in the remainder of this section, we use the concept of SoC, which expresses the battery's unit-independent state of charge relative to its nominal capacity, i.e., a SoC of 0% corresponds to an empty and a SoC of 100% to a full battery.

Most electric vehicles use Lithium-ion (Li-Ion) batteries for energy storage. These are commonly charged with a constant current - constant voltage (CC-CV) charging scheme to prevent critically damaging the battery's internals by overcharging. This process is best understood using the battery model developed in Tremblay, Dessaint, and Dekkiche (2007) and Zang et al. (2019), which is specifically tailored to ECV applications. Tremblay, Dessaint, and Dekkiche model the battery as a controlled voltage source in series with a resistor (see Figure 2), which allows expressing the dynamics of the charging process as:

$$V_{term}(\texttt{SoC}) \coloneqq V_{OC}(\texttt{SoC}) + R \cdot I. \tag{1}$$

Equation (1) states the relationship between terminal voltage ($V_{term}(\texttt{SoC})$), which refers to the voltage measured across the battery's terminals during the charging process, the open-circuit voltage ($V_{OC}(\texttt{SoC})$), which corresponds to the terminal voltage in a disconnected state, and the charging current I. The battery's internal resistance is denoted by R and varies with several exogenous factors, e.g., temperature, load, and battery age. For the sake of simplicity, we assume this resistance to be constant (cf. Pelletier et al. (2017)).

The open circuit voltage, $V_{OC}(\texttt{SoC})$, increases (non-linearly) with the battery's SoC and is often

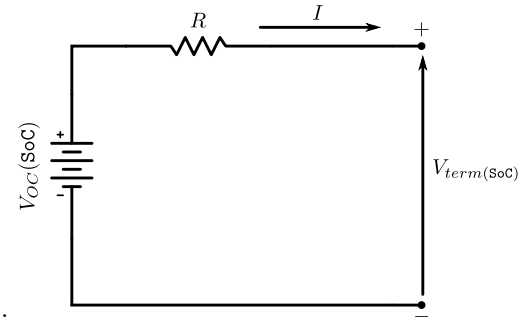

Figure 2: Circuit diagram of the battery model developed in Tremblay, Dessaint, and Dekkiche (2007)

used as an indicator of the battery's charge level. In practice, $V_{OC}(\texttt{SoC})$ is often approximated using Equation (2), parameterized with experimental data (cf. Marra et al. 2012, Pelletier et al. 2017):

$$V_{OC}(\texttt{SoC}(t)) \coloneqq E_0 - \frac{K}{\texttt{SoC}(t)} + A\exp(-BQ(1-\texttt{SoC}(t))). \tag{2}$$

Here, E_0 denotes the battery's constant voltage, Q corresponds to the battery'sä capacity in ampere-hours, A and B are parameters, and K is the polarization voltage. To prevent damaging the battery's electrodes, the charging current I and the terminal voltage $V_{term}(\texttt{SoC})$ must remain within charger and battery-dependent bounds $I_{\max}$ and $V_{term}^{\max}$, respectively. Usually, the maximum terminal voltage $V_{term}^{\max}$ lies well below $V_{term}(100\%) = V_{OC}(100\%) + R \cdot I_{\max}$ and is hence exceeded before the battery is fully charged. To respect this voltage threshold, the CC-CV charging scheme is as follows: first the charging current I is held constant at $I_{\max}$ in the *CC* charging phase until $V_{term}(\texttt{SoC})$ reaches $V_{term}^{\max}$, at which point the *CV* charging phase begins. Here, the charging current I is steadily reduced such that $V_{term}(\texttt{SoC})$ remains at but does not exceed $V_{term}^{\max}$. The constant voltage (CV) phase ends when the charging current drops below manufacturer recommendations. The SoC evolution over time during CC-CV charging is thus non-linear and concave.

C.2. Modeling CC-CV charging

We capture the charger-specific non-linear behavior of the CC-CV charging process in charging functions $\Phi_f(\tau)$, which map the time spent charging at charger f to the resulting SoC when charging with an initially empty battery. In what follows, we describe how to derive $\Phi_f(\tau)$ from battery and charger specifications. Let $I_{\max}^f$ be the maximum charging current of charger f and τ_{CV}^f be the point in time where the CV phase of charger f begins. We can then express Φ_f using auxiliary functions $\Phi_f^{CC}(\tau)$ and $\Phi_f^{CV}(\tau)$, which correspond to the CC and CV phases of the charging process, respectively, in Equations (3a)-(3d):

$$\Phi_f^{CC}(\tau) \coloneqq \Phi_f(0) + \frac{I_{\max}^f \cdot \tau}{Q}, \tag{3a}$$

$$V_{CC} \coloneqq V_{OC}(\texttt{SoC}(\tau)) + R \cdot 3600 \cdot Q \cdot \frac{\partial \Phi_f^{CV}(\tau)}{\partial \tau}, \tag{3b}$$

$$\frac{\partial \Phi_f^{CV}(\tau)}{\partial \tau} \coloneqq \frac{V_{CC} - V_{OC}(\Phi_f^{CV}(\tau))}{R \cdot 3600 \cdot Q}, \tag{3c}$$

$$\widetilde{\Phi}_f(\tau) \coloneqq \begin{cases} \Phi_f^{CC}(\tau) & \text{if } \tau \leq \tau_{CV}^f \\ \Phi_f^{CV}(\tau) & \text{otherwise.} \end{cases} \tag{3d}$$

Solving Equations (3a)-(3d), we obtain an accurate model of the charging process, which we can easily incorporate into our planning problem. We note that $\widetilde{\Phi}_f$ is concave for realistic charger models and, without loss of generality, extend the definitions of $\widetilde{\Phi}_f$ and $\widetilde{\Phi}_f^{-1}$ to avoid edge cases in the main body of this work. Equations (4) and (5) state the final definitions.

$$\Phi_f(\tau) \coloneqq \begin{cases} \widetilde{\Phi}_f & \text{if } \tau \leq 0 \\ \widetilde{\Phi}_f(\tau_{\max}) & \text{if } \tau \geq \tau_{\max} \\ \widetilde{\Phi}_f(\tau) & \text{otherwise.} \end{cases} \tag{4}$$

$$\Phi_f^{-1}(\beta) \coloneqq \begin{cases} 0 & \text{if } \beta \leq \widetilde{\Phi}_f(0) \\ \tau_{\max} & \text{if } \beta \geq \widetilde{\Phi}_f(\tau_{\max}) \\ \widetilde{\Phi}_f^{-1}(\beta) & \text{otherwise.} \end{cases} \tag{5}$$

Here, $\tau_{\max}$ represents the point in time at which the charging current falls below manufacturer recommendations. We assume that $\tau_{\max}$ is finite, such that there exists some $\tau_{\max} > 0$ with $\Phi_f(\tau_{\max}) = \mathtt{SoC}_{\max}$. Finally, we note that Φ_f are continuous functions and that the main body of this work, in line with Pelletier et al. (2017), Montoya et al. (2017), and Froger et al. (2019), instead uses Φ_f to refer to the piecewise linear approximation of Φ_f.

C.3. Battery degradation

The CC-CV charging scheme prevents critically damaging a battery through overcharging. However, overcharging is not the only cause of accelerated degradation. More precisely, the magnitude of battery degradation resulting from (dis-)charging depends on (endogenous) factors such as cycle depth, charging current, and residual SoC. Hence, different charge scheduling decisions have different impacts on battery life. In fact, there exists a trade-off between utilization and battery degradation, that an operator can use to her advantage. Capturing this trade-off requires quantifying the impact of charge scheduling decisions on battery health in an analytical model. Such models take one of two approaches: they either model battery wear based on the underlying electro-chemical processes, or pursue an empirical approach based on experimental data (cf. Reniers, Mulder, and Howey 2019). As data required to parameterize the former is often unavailable and may vary between individual cells, we rely on an empirical approach to quantify battery degradation. To this end, we follow the approach from Pelletier, Jabali, and Laporte (2018) and base our model on the work of Han, Han, and Aki (2014).

Han, Han, and Aki (2014) relate battery price to cycle life specifications supplied by manufacturers, specifically to the depth of discharge - achievable cycle count (DOD-ACC) curve. Each point on the DOD-ACC curve, $ACC(D)$, corresponds to the number of cycles achievable before the battery becomes unusable when it is cycled at the respective depth of discharge (DoD). For instance, $ACC(20\%) = 2500$ indicates that the battery can be discharged from 100% to 80% and then recharged back to 100% SoC 2500 times before capacity and power fade render it ineffective.

The DOD-ACC function establishes a relationship between battery life and price: dividing the battery price by the total energy transferred over $ACC(D)$ cycles gives the average wear cost of (dis-)charging when cycling the battery at a DoD of D, denoted $AWC(D)$. However, the average wear cost function is only of limited use as it is only valid if the battery is always cycled in the same fashion, i.e., from 100% SoC to $1 - D$ and back to 100%. Han, Han, and Aki (2014) address this issue

by combining n (equidistant) points on the DOD-ACC curve according to the following methodology: let $S \coloneqq [S_1, \dots, S_n]$ be the SoC values corresponding to the given DOD-ACC points and let

$$Q(s) \coloneqq ACC(1-s) \cdot 2 \cdot (1-s) \cdot C \tag{6}$$

denote the total amount of energy transferred when cycling a battery with capacity C to a SoC of s. For the highest SoC segment S_n, the battery price c_{bat} must equal the wear cost $\widetilde{\Upsilon}(S_n)$ of energy charged on the segment $[S_n, 100\%]$, multiplied by the total amount of energy transferred over the battery's lifespan when cycling at $D = 1 - S_n$. Equation (7) formalizes this relationship:

$$c_{\text{bat}} = Q(S_n) \cdot \widetilde{\Upsilon}(S_n). \tag{7}$$

Each charging cycle at a DoD of $1 - S_{n-1}$ also cycles the battery at $1 - S_n$. Hence, the average wear cost must be at least $\widetilde{\Upsilon}(S_n)$. Formally, we have $AWC(1 - S_{n-1}) = \widetilde{\Upsilon}(S_n) + \epsilon$ for some $\epsilon > 0$. We thus have $AWC(1 - S_i) = \sum_{j=i}^{n} \widetilde{\Upsilon}(S_j)$ by induction, i.e., the average wear cost corresponds to the sum of wear costs incurred on all utilized segments. Hence, we can generalize Equation (7) to Equation (8):

$$c_{\text{bat}} = Q(S_i) \cdot (\sum_{j=i}^{n} \widetilde{\Upsilon}(S_j)). \tag{8}$$

Equation (8) yields a linear equation system of size n, which can be solved for $\widetilde{\Upsilon}(s)$ at discrete points $s \in \{S_1, \dots, S_n\}$ (cf. Han, Han, and Aki 2014). Setting $\widetilde{\Upsilon}(s) \coloneqq \widetilde{\Upsilon}(S_i)$ for $s \in [S_i, S_{i+1}], 0 \leq i < n$ finally yields a piecewise constant function, called the *wear density function*, which gives the unit cost of charging at a certain SoC. We utilize this function to compute the *(cumulative) wear density function*, denoted by $\Upsilon : \texttt{SoC} \mapsto \texttt{cost}$. Specifically, we obtain Υ by integrating $\widetilde{\Upsilon}$, which yields a convex piecewise linear function stating the total cost of charging an initially empty battery up to a certain SoC.

Appendix D: Implementation details

Algorithm 1 details our label-setting search procedure. The algorithm relies on several data structures: first, it maintains a set of settled ($\mathcal{L}_v^{set}$) and unsettled ($\mathcal{L}_v^{uns}$) labels for each vertex $v \in \mathcal{V}^k$. These keep track of already developed paths and collect candidates for expansion, respectively. To establish the label-setting property of our algorithm, we store vertices v with unsettled labels, i.e., potential candidates for expansion, in a priority queue $\mathcal{Q}$. This queue orders vertices according to the cost of the cheapest unsettled label at the respective vertex, formally, $\min_{\ell \in \mathcal{L}_v^{uns}} c_{\min}(\psi_\ell) \geq \min_{\ell \in \mathcal{L}_{v'}^{uns}} c_{\min}(\psi_\ell) \Rightarrow v \succeq_{\mathcal{Q}} v'$ for $v, v' \in \mathcal{Q}$. We break ties according to the vertex's period index in descending order such that we prefer vertices closer to the sink node.

We initialize $\mathcal{Q}$ with the source vertex and root label (Lines 2-3). The main body of the algorithm (Lines 4-21) iteratively extracts labels from $\mathcal{Q}$ (Lines 5-6) and propagates these along all adjacent arcs (Lines 11-16). We propagate extracted labels $\ell \in \mathcal{L}_i$ along idle and service arcs (i, j) according to

Algorithm 1: Label setting search

1 **Initialization:**
2 $\mathcal{L}^{uns}_{s^-} \coloneqq \{\ell_{s^-}\}$;
3 $\mathcal{Q} \coloneqq \{s^-\}$;
4 **while** $\mathcal{Q}$.*notEmpty()* **do**
5 $\quad i \coloneqq \mathcal{Q}$.pop();
6 $\quad \ell \coloneqq$ extract_min($\mathcal{L}^{uns}_i$);
7 $\quad$ **if** $i = s^+$ **then**
8 $\quad\quad$ **return** $c_{\min}(\psi_\ell)$;
9 $\quad$ **if** $\exists \ell' \in \mathcal{L}^{set}_i, \ell' \succeq \ell$ **then**
10 $\quad\quad$ **continue**;
11 $\quad$ **for** $(i,j) \in \mathcal{E}^k$ **do**
12 $\quad\quad$ **if** $(i,j) \notin \mathcal{E}^k_{\mathcal{F}}$ **then**
13 $\quad\quad\quad \mathcal{L}_{new} \coloneqq \{\ell \underset{(i,j)}{\leftarrow} /\}$;
14 $\quad\quad$ **else**
$\quad\quad\quad$ // Track charging decisions in period $p(i)$
15 $\quad\quad\quad \mathcal{L}_{new} \coloneqq \{\ell \overset{f(i)}{\underset{(i,j)}{\leftarrow}} c \mid c \in \mathcal{B}(\psi_\ell)\}$;
$\quad\quad\quad$ // Charge for $\tau = \xi$ in $p(i)$
16 $\quad\quad\quad \mathcal{L}_{new} \coloneqq \mathcal{L}_{new} \cup \{\ell \underset{(i,j)}{\leftarrow} \xi\}$;
17 $\quad\quad$ remove_set_dominated($\mathcal{L}_{new}$);
$\quad\quad$ // Enqueue feasible labels
18 $\quad\quad$ **for** $\ell' \in \mathcal{L}_{new}$ **do**
19 $\quad\quad\quad$ **if** *feasible*(ℓ') **then**
20 $\quad\quad\quad\quad$ insert($\mathcal{L}^{uns}_j, \ell'$);
21 $\quad$ insert($\mathcal{L}^{set}_i, \ell$);
22 **return** *infeasible*;

$c_{i,j}$, $q_{i,j}$, and $\vartheta_{i,j}$. Charging arcs require special treatment: here, it is possible to either commit to a charging decision at a previously visited station vertex i' to then track charging trade-offs at station vertex i, or to commit to charging at i, continuing to track decisions at i'. Line 15 handles the former case and creates a label for each non-dominated charging decision at the station vertex i' tracked by ℓ so far, i.e., fixes the amount of charge replenished at i', and thus the arrival SoC at i to some value. Line 16 handles the latter case, i.e., spawns a label that charges at i *without* forcing a decision at the tracked station i'. This fixes the amount of time spent charging at i to some value. Note that ignoring the charging opportunity at i corresponds to visiting the respective garage vertex and is thus not explicitly considered. We prune the set of generated labels according to our set-based dominance criterion (cf. Definition 2) in Line 17.

Lines 18-20 insert feasible labels into $\mathcal{L}_j^{uns}$, i.e., track potential candidates for expansion at vertex j, updating the vertex queue accordingly. Finally, we settle the original label at vertex i for future dominance checks. The algorithm terminates when a label is extracted at the sink (Line 8), or no unsettled labels remain.

We implement $\mathcal{L}_i^{uns}$ as a min-heap and key labels by minimum cost. We postpone pairwise dominance checks against already settled labels to label extraction (Line 9). This lazy approach serves two purposes: first, it avoids superfluous dominance checks for labels never considered during the search; second, it delays dominance checks as much as possible to maximize the number of candidates for domination.

We further rely on two techniques to speed up dominance checks: first, we keep $\mathcal{L}_i^{set}$ sorted by maximum reachable SoC. This allows skipping superfluous dominance checks against settled labels with a lower maximum SoC. Second, we maintain a hash table of settled and unsettled labels at each vertex. We probe this hash table and abort the dominance check if an equivalent label is found. These strategies minimize the number of (explicit) dominance checks required to maintain our dominance invariant.

Appendix E: Compact formulation

In the following, we model our planning problem as a mixed integer program, which we state as a shortest path problem on the time-expanded network presented in Section 3.1. MIP 1 comprises the following decision variables: binary variable $x_{i,j}^k$ indicates that vehicle k traverses arc (i,j). Variables $\lambda_{v,b}^{k,in}$ and $\lambda_{v,b}^{k,out}$ model charging operations as piecewise linear functions. To this end, continuous variables $\lambda_{v,b}^{k,in}$ and $\lambda_{v,b}^{k,out}$ are convex multipliers associated with the breakpoints of the respective piecewise linear charging functions, i.e., give the contribution of each breakpoint to the function value. We establish a Special-Ordered Set of Type 2 (SOS2) relationship between variables associated with the same vertex and vehicle. Variables $\mu_{v,b}^{k,in}$ and $\mu_{v,b}^{k,out}$ model the WDF analogously. We use continuous variables β_v^k and γ_v^k to track the arrival SoC and total amount of energy replenished by vehicle k at vertex $v \in \mathcal{V}^k$. With the notation summarized in Table 1, our mixed integer program (MIP) is as follows.

$$\min \sum_{k \in \mathcal{K}} \sum_{v \in \mathcal{V}_{\mathcal{F}}^k} \gamma_v^k \cdot e_{p(v)} + \rho_v^k \tag{1.1}$$

$$\sum_{(i,j) \in \delta^-(s^-)} x_{i,j}^k = 1 \qquad k \in \mathcal{K} \tag{1.2}$$

$$\sum_{(i,j) \in \mathcal{E}_\vartheta^k} x_{(i,j)}^k \geq 1 \qquad \vartheta \in \Theta_k, k \in \mathcal{K} \tag{1.3}$$

$$\sum_{(i,j) \in \delta^+(v)} x_{i,j}^k - \sum_{(i,j) \in \delta^-(v)} x_{i,j}^k = 0 \qquad v \in \mathcal{V}^k \setminus \{s^-, s^+\}, k \in \mathcal{K} \tag{1.4}$$

$$\beta_i^k + q_{i,j} + \gamma_i^k \geq \beta_j^k - (1 - x_{i,j}^k) \cdot \mathtt{SoC}_{\max} \qquad \forall (i,j) \in \mathcal{E}^k, k \in \mathcal{K} \tag{1.5}$$

$\mathcal{V}^k$	set of vertices
$\mathcal{V}^k_{\mathcal{F}}$	set of charger vertices
$\mathcal{V}^k_f$	set of vertices associated with charger f
$\delta^+(v)$	set of incoming arcs at vertex v
$\delta^-(v)$	set of outgoing arcs at vertex v
$\mathcal{E}^k_{\mathcal{F}}$	set of charging arcs
$\mathcal{E}^k_{\Theta_k}$	set of service arcs
e_p	energy cost in period p
$q_{i,j}$	charge consumption of arc (i,j)
$c_{i,j}$	cost of arc (i,j)
$\mathcal{F}$	set of chargers
C_f	charger capacity for $f \in \mathcal{F}$
$\mathcal{B}(f)$	breakpoints of the linearized charging function
$q_{f,b}$	SoC associated with breakpoint $b \in \mathcal{B}(f)$
$t_{f,b}$	Time associated with breakpoint $b \in \mathcal{B}(f)$
$\mathcal{B}(\Upsilon)$	breakpoints of the (cumulative) wear density function (WDF)
$q_{\Upsilon,b}$	SoC associated with breakpoint $b \in \mathcal{B}(\Upsilon)$
$c_{\Upsilon,b}$	Costs per kWh associated with breakpoint $b \in \mathcal{B}(\Upsilon)$
$\mathcal{P}$	set of periods in the planning horizon
$\mathcal{K}$	set of vehicles
$\mathtt{SoC}_{\max}$	maximum battery charge level (SoC)
$\mathtt{SoC}_{\min}$	minimum battery charge level (SoC)
β^k_v	SoC with which vehicle k arrives at vertex v
γ^k_v	SoC charged/discharged at vertex v
ρ^k_v	battery wear cost incurred by charging at v
$x^k_{i,j}$	binary variable, indicating whether vehicle k traverses arc (i,j) ($x^k_{i,j}=1$) or not ($x^k_{i,j}=0$)
$\lambda^{k,in}_{v,b}$	Convex multipliers binding entry SoC to $\Phi_{f(v)}$
$\lambda^{k,out}_{v,b}$	Convex multipliers binding exit SoC to $\Phi_{f(v)}$
$\mu^{k,in}_{v,b}$	Convex multipliers binding entry SoC to Υ
$\mu^{k,out}_{v,b}$	Convex multipliers binding exit SoC to Υ

Table 1: Parameters and variables of the compact formulation.

$$\beta^k_i + q_{i,j} + \gamma^k_i \leq \beta^k_j + (1 - x^k_{i,j}) \cdot \mathtt{SoC}_{\max} \qquad \forall (i,j) \in \mathcal{E}^k, k \in \mathcal{K} \quad (1.6)$$

$$\mathtt{SoC}_{\min} \leq \beta^k_v \leq \mathtt{SoC}_{\max} \qquad v \in \mathcal{V}^k, k \in \mathcal{K} \quad (1.7)$$

$$\beta^k_{s^-} = \mathtt{SoC}_{\min} \qquad k \in \mathcal{K} \quad (1.8)$$

$$\sum_{b \in \mathcal{B}(f(v))} \lambda^{k,in}_{v,b} \cdot q_{f(v),b} = \beta^k_v \qquad v \in \mathcal{V}^k_{\mathcal{F}}, k \in \mathcal{K} \quad (1.9)$$

$$\sum_{b \in \mathcal{B}(f(v))} \lambda^{k,in}_{v,b} = 1 \qquad v \in \mathcal{V}^k_{\mathcal{F}}, k \in \mathcal{K} \quad (1.10)$$

$$\sum_{b \in \mathcal{B}(f(v))} \lambda^{k,out}_{v,b} \cdot q_{f(v),b} - \sum_{b \in \mathcal{B}(f(v))} \lambda^{k,in}_{v,b} \cdot q_{f(v),b} = \gamma^k_v \qquad v \in \mathcal{V}^k_{\mathcal{F}}, k \in \mathcal{K} \quad (1.11)$$

$$\sum_{b \in \mathcal{B}(f(v))} \lambda^{k,out}_{v,b} = 1 \qquad v \in \mathcal{V}^k_{\mathcal{F}}, k \in \mathcal{K} \quad (1.12)$$

$$\sum_{b \in \mathcal{B}(f(v))} \lambda^{k,out}_{v,b} \cdot t_{f(v),b} - \sum_{b \in \mathcal{B}(f(v))} \lambda^{k,in}_{v,b} \cdot t_{f(v),b} \leq \xi \cdot \sum_{(i,j) \in \delta^-(v)} x^k_{i,j} \qquad v \in \mathcal{V}^k_f, k \in \mathcal{K} \quad (1.13)$$

$$\sum_{b\in\mathcal{B}(\Upsilon)} \mu^{k,in}_{v,b} \cdot q_{\Upsilon,b} = \beta^k_v \qquad v\in\mathcal{V}^k_{\mathcal{F}}, k\in\mathcal{K} \quad (1.14)$$

$$\sum_{b\in\mathcal{B}(\Upsilon)} \mu^{k,in}_{v,b} = 1 \qquad v\in\mathcal{V}^k_{\mathcal{F}}, k\in\mathcal{K} \quad (1.15)$$

$$\sum_{b\in\mathcal{B}(\Upsilon)} \mu^{k,out}_{v,b} \cdot q_{\Upsilon,b} - \sum_{b\in\mathcal{B}(f(i))} \mu^{k,in}_{v,b} \cdot q_{\Upsilon,b} = \gamma^k_v \qquad v\in\mathcal{V}^k_{\mathcal{F}}, k\in\mathcal{K} \quad (1.16)$$

$$\sum_{b\in\mathcal{B}(\Upsilon)} \mu^{k,out}_{v,b} = 1 \qquad v\in\mathcal{V}^k_{\mathcal{F}}, k\in\mathcal{K} \quad (1.17)$$

$$\sum_{b\in\mathcal{B}(\Upsilon)} \mu^{k,out}_{v,b} \cdot c_{\Upsilon,b} - \sum_{b\in\mathcal{B}(\Upsilon)} \mu^{k,in}_{v,b} \cdot c_{\Upsilon,b} = \rho^k_v \qquad v\in\mathcal{V}^k_{f}, k\in\mathcal{K} \quad (1.18)$$

$$\sum_{k\in\mathcal{K}} \sum_{(i,j)\in\delta^-(v)} x^k_{i,j} \leq C_{f(v)} \qquad \forall v\in\bigcup_{k\in\mathcal{K}} \mathcal{V}^k_{\mathcal{F}} \quad (1.19)$$

$$x^k_{i,j} \in \{0,1\} \qquad (i,j)\in\mathcal{E}, k\in\mathcal{K} \quad (1.20)$$

$$\beta^k_v, \gamma^k_v, \rho^k_v \geq 0 \qquad v\in\mathcal{V}^k, k\in\mathcal{K} \quad (1.21)$$

$$\forall b\in\mathcal{B}(f(v)) : \lambda^{k,in}_{v,b}, \lambda^{k,out}_{v,b} \in SOS2 \qquad v\in\mathcal{V}^k_{\mathcal{F}}, k\in\mathcal{K} \quad (1.22)$$

$$\forall b\in\mathcal{B}(\Upsilon) : \mu^{k,in}_{v,b}, \mu^{k,out}_{v,b} \in SOS2 \qquad v\in\mathcal{V}^k_{\mathcal{F}}, k\in\mathcal{K} \quad (1.23)$$

The objective function (1.1) minimizes the total cost of the charging schedule, i.e., the sum of energy costs and battery wear incurred. Constraints (1.2) and (1.3) enforce an outgoing and incoming arc at the source and sink nodes, respectively. Constraints (1.4) set up flow conservation on all other vertices. Constraints (1.5)-(1.6) propagate the SoC. The concaveness of the WDF requires strict equality. Consumption and charging operations are captured with $q_{i,j}$ and γ^k_i, respectively. Constraints (1.7) ensure that manufacturer SoC bounds are respected. Constraints (1.8) initialize $\beta^k_{s^-}$. Constraints (1.9-1.12) model charging operations as piecewise linear functions. Constraints (1.13) limit the maximum SoC rechargeable at station nodes, i.e., ensure that the charging rate is respected, and establish a link between $x^k_{i,j}$ and γ^k_v, such that charging can occur only if the station node is visited. Constraints (1.14)-(1.18) model battery degradation similarly. Constraints (1.19) limit the number of simultaneous charging operations at each charger. Finally, Constraints (1.20)-(1.23) state the domain of the decision variables and establish SOS2 sets.

Appendix F: Benchmark instance generation

We choose a discretization step size of 30 minutes and draw period energy prices uniformly from the interval $[0.5, 1.0]$ (€). We further assume a battery capacity of 80 kWh with $\mathtt{SoC}_{\min} \coloneqq 0\%$ and $\mathtt{SoC}_{\max} \coloneqq 100\%$. To avoid biases in our numerical study, we generate charging functions Φ_f and the WDF randomly according to the following procedure: Given parameters n, $\chi_{\min}, \chi_{\max}$, and ν, which correspond to the number of segments, minimum slope, maximum slope, and upper bound respectively, we assign a random weight w_i, and a slope drawn from interval $[\chi_{\min}, \chi_{\max}]$ to each segment i. We then sort the segments by slope in descending (ascending) order such that the resulting function is

convex (concave) for WDF and charging functions, respectively. We transform the piecewise linear functions generated in this fashion to valid WDF and charging functions by scaling each segment i to span $\nu \cdot \frac{w_i}{\sum_{j\in[1,n]} w_j}$ on the SoC and time axes. We generate the WDF with $\chi_{\min} \coloneqq 0.1$, $\chi_{\max} \coloneqq 0.8$, and $\nu \coloneqq 80$. We use durations $\nu \coloneqq [150, 60, 90, 120, 75, 135]$ to generate chargers, such that fully charging the battery using the i^{th} charger takes ν_i minutes. Unless otherwise specified, we distribute charger capacity evenly across all available chargers. Finally, we generate a set of three operations for each day and vehicle. Each service operation consumes 50% of the battery capacity, leading to a total discharge of 120 kWh per day and vehicle. We distribute operation departure times randomly such that vehicles spend a minimum of one hour before each operation at the depot, and center the departure time windows according to the static case. To ensure that the generated instances are comparable, we use independently seeded random engines for each parameter, such that the set of service operations of a one day instance is a subset of the service plan of the two and three-day instances generated from the same seed.

Appendix G: Data used in the example

SoC	Cost	Unit cost
0	0	-
2	1	0.5
7	7	1.2

Table 2: Wear density function.

Arc	Consumption ($q_{i,j}$)	Fixed cost ($c_{i,j}$)	Energy cost at origin
(s^-, v_f)	0	2	0
(v_f, v_2)	0	0	2.5
(v_2, v_3)	1.5	0	0
(v_3, v_g)	0	0	0
(v_g, v_5)	0	0	0.75
$(v_5, s^+)(1)$	0	3.5	0
$(v_5, s^+)(2)$	0	4.25	0

Table 3: Arcs of the time expanded network.

f			g		
Time	SoC	Rate	Time	SoC	Rate
0	0	-	0	0	-
6	2	0.3333	2.5	2	0.8
24.5	7	0.2707	12.25	7	0.5128

Table 4: The charging functions used.

f			g		
Cost	SoC	Rate	Cost	SoC	Rate
0	0	-	0	0	-
6	2	0.3333	2.5	2	0.8
24.5	7	0.2702	12.25	7	0.5128

Table 5: The station cost profiles.

Cost profile	Segments			
$\psi_{\ell_{s^-}}$	$[-\infty, 0.0) \to [-\infty, -\infty]$	$[0.0, \infty) \to [0.0, 0.0]$		
$\psi_{\ell_{v_f}}$	$[-\infty, 2.0) \to [-\infty, -\infty]$	$[2.0, \infty) \to [0.0, 0.0]$		
$\psi_{\ell_{v_2}}$	$[-\infty, 2.0) \to [-\infty, -\infty]$	$[2.0, 8.0) \to [0.0, 2.0]$	$[8.0, 11.7) \to [2.0, 3.0)$	$[11.7, \infty] \to [3.0, 3.0]$
$\psi_{\ell_{v_3}}$	$[-\infty, 6.5) \to [-\infty, -\infty]$	$[6.5, 8.0) \to [0.0, 0.5]$	$[8.0, 11.7) \to [0.5, 1.5)$	$[11.7, \infty] \to [1.5, 1.5]$
$\psi_{\ell_{v_g}}$	$[-\infty, 6.5) \to [-\infty, -\infty]$	$[6.5, 8.0) \to [0.0, 0.5]$	$[8.0, 11.7) \to [0.5, 1.5)$	$[11.7, \infty] \to [1.5, 1.5]$
$\psi^1_{\ell_{v_5}}$	$[-\infty, 6.5) \to [-\infty, -\infty]$	$[6.5, 9.0) \to [0.0, 2.0]$	$[9.0, 12.9) \to [2.0, 4.0)$	$[12.9, \infty] \to [4.0, 4.0]$
$\psi^2_{\ell_{v_5}}$	$[-\infty, 12.9) \to [-\infty, -\infty]$	$[12.9, 14.75) \to [4.0, 4.5]$	$[14.75, 19.15) \to [4.5, 5.5)$	$[14.75, \infty] \to [5.5, 5.5]$
$\psi^3_{\ell_{v_5}}$	$[-\infty, 8.0) \to [-\infty, -\infty]$	$[8.0, 9.875) \to [0.5, 2.0]$	$[9.875, 14.75) \to [2.0, 4.5)$	$[14.75, \infty] \to [4.5, 4.5]$
$\psi^4_{\ell_{v_5}}$	$[-\infty, 11.7) \to [-\infty, -\infty]$	$[11.7, 12.325) \to [1.5, 2.0]$	$[12.325, 19.15) \to [2.0, 5.5)$	$[12.325, \infty] \to [5.5, 5.5]$
$q_{(v_5, s^+)} = 4.25$				
$\psi^1_{\ell_{s^+}}$	$[-\infty, 11.925) \to [-\infty, -\infty]$	$[11.925, 12.9) \to [0.0, 0.5]$	$[12.9, \infty) \to [0.5, 0.5)$	
$\psi^2_{\ell_{s^+}}$	$[-\infty, 12.9) \to [-\infty, -\infty]$	$[12.9, 14.75) \to [0.5, 1.0]$	$[14.75, 19.15) \to [1.0, 2.0)$	$[14.75, \infty] \to [2.0, 2.0]$
$q_{(v_5, s^+)} = 3.5$				
$\psi^2_{\ell_{s^+}}$	$[-\infty, 13.825) \to [-\infty, -\infty]$	$[13.825, 14.75) \to [0.0, 0.25]$	$[14.75, 19.15) \to [0.25, 1.25)$	$[14.75, \infty] \to [1.25, 1.25]$
$\psi^3_{\ell_{s^+}}$	$[-\infty, 14.2625) \to [-\infty, -\infty]$	$[14.2625, 14.75) \to [0.0, 0.25]$		$[14.75, \infty] \to [0.25, 0.25]$

Table 6: Cost profiles created in the example.